

## Evaluation of ductility and response modification factor in moment-resisting steel frames with CFT columns

Seyed Sh. Hashemi<sup>\*1</sup>, Kabir Sadeghi<sup>2a</sup>, Mohammad Vaghefi<sup>1b</sup> and Kaveh Shayan<sup>3c</sup>

<sup>1</sup>Department of Civil Engineering, Persian Gulf University, Shahid Mahini Street, P.O. Box: 75169-13817, Bushehr, Iran

<sup>2</sup>Department of Civil Engineering, Near East University, ZIP Code: 99138, Nicosia, North Cyprus, Mersin 10, Turkey

<sup>3</sup>Department of Civil Engineering, Islamic Azad University of Bushehr, Varzesh Street, P.O. Box: 75196-1955, Bushehr, Iran

(Received July 7, 2016, Revised May 24, 2017, Accepted May 25, 2017)

**Abstract.** One of the methods to strengthen the structures against the seismic lateral loading is the employment of the composite columns. A concrete-filled tube (CFT) has the cumulative advantages of steel and concrete. Concrete-filled steel tube columns have been widely used in the moment-resisting frame (MRF) structures, located in both non-seismic zones and high-risk seismic zones. In this paper, the results of studies on two important seismic parameters of ductility and the response modification factor (RMF) of the MRFs with CFT columns are submitted. While the studies are carried out, the effects of span length-story height ratio, the strength of materials and seismic behavior of MRFs are considered. In this regard, the ductility, RMF and the strength of 36 models of the steel MRFs with CFTs are analyzed. The fiber plastic hinges numerical simulation and pushover analysis method are used in the calculations. Based on the obtained results, the RMFs suitable for the 5-, 10- and 15- story frames are proposed.

**Keywords:** response modification factor; ductility, CFT column, pushover analysis, fiber plastic hinge

### 1. Introduction

Moment-resisting frames (MRFs) have been traditionally used for the lateral-force resisting systems in the area of the high seismicity because they have significant potential for large ductility under seismic loading (Park *et al.* 2011).

The complex way of thinking and application of the composite components was first made possible by ASHTO criteria in 1944. When it comes to the buildings, AISC criteria verified the permission of mixed floor application in the buildings in 1952 (McCormack 2007). Recently, this type of MRF has been employed in composite constructions (Park *et al.* 2011). The CFT columns are often used in the simple frame building systems along with the shear walls to resist the lateral loading. In Fig. 1 some examples of the composite columns are shown (Kuranovas and Kvedaras 2007).

Concrete-filled steel columns are the columns with tubular or canned cross section, filled entirely with concrete. In the recent years, CFT structures have been widely used in the tall buildings and the arch bridges,

particularly, in the far-east region such as China and Japan (Xiao *et al.* 2005). Due to the advantageous properties of steel such as high tensile strength and ductility, along with the suitable compressive strength of concrete, this composite element has been considered as a good structural element. In this fashion, the steel surrounds the concrete and significantly increases the stiffness and strength of the element. The filled concrete enforces the local buckling in the tube and increases the ductility. The tube prohibits excessive concrete spalling (Schneider and Kramer 2004). Moreover, application of CFT columns reduces the cost. High shear strength, high energy absorption capacity, confining the concrete and protection of the concrete surface are some of the other advantages of CFT column application. Various researches have been performed on the ductility and the response modification factor (RMF) of CFT columns. Varma *et al.* (2004) investigated the seismic behavior of square shaped CFT columns with high strength under the fixed axial force and rotating lateral load. They also studied the effects of dimension-thickness ratio, the yield stress of the steel and axial load on the behavior (stiffness, strength, ductility and the absorbed energy) of the square shaped CFT columns. In their study, the ductility factor was obtained 3.2 to 5.8 for different cases. To investigate the seismic behavior of the tubular structures filled with concrete, Jiango *et al.* (2006), performed a static pushover analysis for a 10-story MRF comprising CFT columns and steel beams. The obtained results indicated that the ductility and the absorbed energy of the composite frame would decrease by the increase of the axial load. Nateghi Elahi *et al.* (2008) examined 12 column samples under compression and the periodically increasing lateral force. They concluded that the ductility of the columns with

\*Corresponding author, Assistant Professor

E-mail: sh.hashemi@pgu.ac.ir

<sup>a</sup>Professor

E-mail: kabirsadeghi@gmail.com

<sup>b</sup>Associated Professor

E-mail: vaghefi@pgu.ac.ir

<sup>c</sup>M.Sc. Graduated Student

E-mail: Kave2788@yahoo.com

circular cross sections is more than those of the octagonal cross sections, and the octagonal ones are more ductile in comparison with the columns having the square cross sections. Lee *et al.* (2010) studied the behavior of the CFT columns under off-axial load, performing the fiber element analysis and the experimental test on eleven CFT column samples with circular cross section. They observed that, for the diameter-thickness ratio higher than 80, the ductility of the circular CFT columns filled with a concrete with a lower strength (30 MPa) was higher than the ductility of the CFT columns filled with the concrete with higher strength (60 MPa). Moreover, Zhang *et al.* (2012) studied the seismic performance of the CFT columns, analyzing the load-displacement hysteretic curves, absorbed energy capability and ductility of the sample. Karamis *et al.* (2016) studied the damage of MRFs with CFT columns and observed that the number of stories, beam strength, material strength and ground motion characteristics, strongly influence on the structural damage. Some other researchers such as Kwon and Jeong (2014), Evirgen *et al.* (2014) and Long *et al.* (2016) focused on local buckling and ultimate strength of the CFT columns, employing the experimental and numerical simulations. Xiamuxi *et al.* (2015) employed an experiment-based verification policy and developed a general FE nonlinear analysis model to analyze the mechanical behavior and the failure mechanism of reinforced concrete-filled tubular steel (RCFT) columns under uniaxial compression. They proposed reasonable stress-strain relationships for confined concrete, reinforcements and steel tube in the model. They also found out a mechanism for shear failure of the concrete core in the numerical simulation and proposed a non-conventional method and equation for evaluating the confinement effect of RCFT. Esfandyary *et al.* (2015) studied the hysteretic behavior of concrete-filled steel tubular (CFT) column connected to I-beam, and implemented a nonlinear finite element (FE) analysis to evaluate the effects of different parameters including the column axial load, beam lateral support, shape and arrangement of stiffeners, stiffness of T-stiffeners, and the number of shear stiffeners. They observed that external T-stiffeners combined with internal shear stiffeners play an important role in the hysteretic performance of CFT columns connected to I-beam. Pokharel *et al.* (2016) performed experimental tests and numerical analyses to study the anchorage behavior of clogged deformed reinforcing bars within concrete-filled circular steel tubes. A series of pull-out tests were conducted using steel tubes with the different diameter to thickness ratios under monotonic and cyclic loading. A comprehensive 3D finite element model was developed to simulate the pull-out tests. They employed a model to conduct parametric studies to investigate the influence of the confinement provided by the steel tube on the infilled concrete. Wan and Zha (2016) presented a new unified design formula for calculating the composite compressive strength of the axially loaded circular concrete-filled double steel tubular (CFDST) short and slender columns. Furthermore, on the basis of the Perry-Robertson formula, they derived the stability factor of CFDST slender columns. An important characteristic of their proposed formulas is

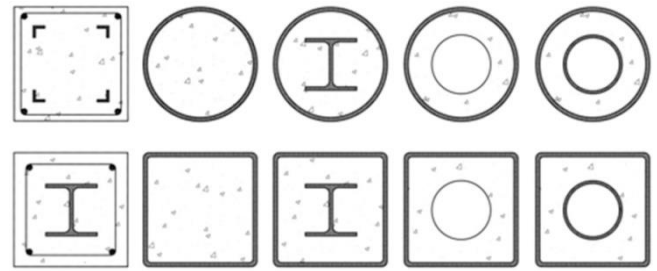


Fig. 1 Composite columns (Kuranovas and Kvedaras 2007)

that they provide a unified formulation for both the plain CFST and CFDST columns relating to the compressive strength or the stability bearing capacity and a set of design parameters.

Since the previous studies have been focused mainly on the small-scale models of single CFT columns; an inadequacy is felt that more investigations are needed to assess the seismic behavior of large and full-scale models with CFT columns. Consequently, in this paper, the results of studies on two important seismic parameters of ductility and RMF ( $R$ ) along with the effects of span length-story height ratio ( $L/H$ ), the strength of materials and seismic behavior of MRFs with CFT columns are submitted.

## 2. Theoretical basis

### 2.1 Employed methods to calculate the response modification factor

It is observed that in the case of strong earthquakes, most of the structures have the nonlinear behavior. Similar to the linear responses, the nonlinear responses are also controllable. In the other words, the horizontal plateau of the base shear-displacement curve could be significantly increased by the use of some methods. By application of some specific measures taken in the design process of hinge composition, the horizontal plateau of the pushover curve, which starts with the formation of the first hinge and continues up to the collapse mechanism, can be enhanced. This means that some measures can be taken somehow that the initial hinge remains safe during the formation of the next hinge and is not crashed. This is the main philosophical point of the seismic design of the structures.

If the structure is designed in a way that it shows sufficient ductility in the places with maximum strain, it would be able to resist the inelastic displacements. This means that the structure would be able to absorb the most of the energy exerted from the earthquake and dissipate it. As it can be seen in Fig. 2, the overall response of a structure with one degree of freedom is depicted in the form of base shear-horizontal displacement curve. In this figure, the response curves of the actual and bilinear idealized responses are shown. The vertical and horizontal axes show the base shear and the relative lateral displacement of the roof, respectively (Tasnimi and Masoumi 2006). According to NEHRP (2001) regulation, the RMF ( $R$ ) is equal to the ratio of elastic base shear ( $V_e$  represents the base shear

calculated according to the linear-elastic response) to the base shear for design ( $V_{design}$ ), therefore

$$R = \frac{V_e}{V_{design}} \quad (1)$$

The design base shear and the elastic base shear of the structures are obtained in accordance with the AISC-LRFD regulations.

The value of response coefficient,  $R$ , for each structural system depends on the parameters of energy absorption capacity, required excess strength, level of indeterminacy in degrees of freedom, the shape of the force-displacement curve, the natural period of the structure, viscosity and frictional attenuation, the type of soil and the properties of the previous earthquakes.

Therefore, according to Fig. 2, the RMFs of the structures in design, using the LRFD method, similar to AISC-LRFD regulation, is

$$R = \frac{V_e}{V_s} = \frac{V_e}{V_y} \times \frac{V_y}{V_s} = R_u \Omega \quad (2)$$

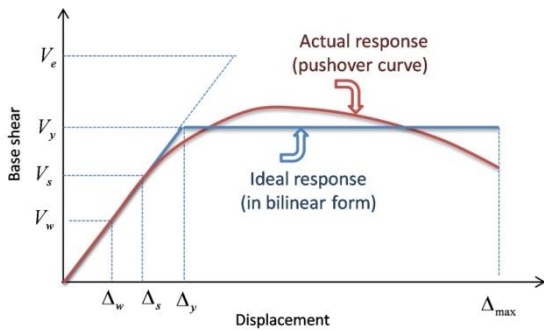


Fig. 2 Effective parameters in seismic design, using pushover curve (Tasnimi and Masoumi 2006)

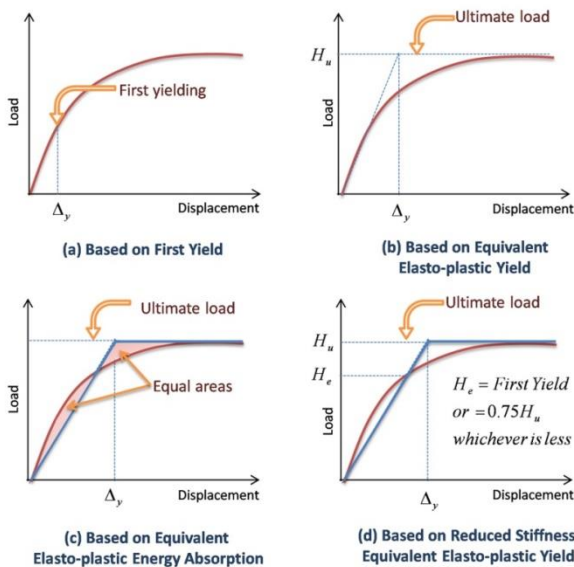


Fig. 3 Alternative definitions of yield displacement (Park 1989)

Where  $R_u$  represents the reduction coefficient due to ductility and  $\Omega$  represents the excess strength coefficient. Other parameters are shown in Fig. 2.

The excess strength coefficient leads to transmit the level of design force from the force level  $V_y$  to the force level  $V_s$ . Therefore, the excess strength coefficient can be written as Eq. (3)

$$\Omega = \frac{V_y}{V_s} = \frac{\Delta y}{\Delta s} \quad (3)$$

Ductility is one of the major properties of the structures in case of earthquake loading. The ductility coefficient ( $\mu$ ) is defined as the ratio of the ultimate displacement ( $\Delta u$ ) to the yield displacement ( $\Delta y$ )

$$\mu = \frac{\Delta u}{\Delta y} \quad (4)$$

The choice of a proper method to evaluate the yield displacement and the ultimate displacement is one of the crucial measures in the seismic design. However, there are different definitions for the condition of the ultimate and yield displacements. Park (1989) itemized the possible definitions for yield and ultimate displacements that have gained considerable recognition worldwide. These definitions are presented in Figs. 3-4 for yield and ultimate

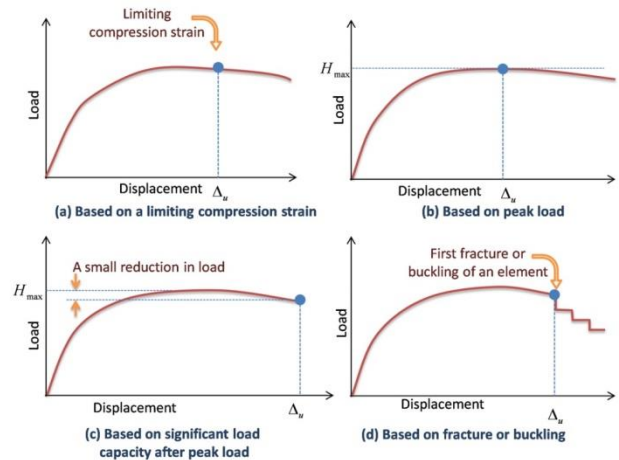


Fig. 4 Alternative definitions of ultimate displacement (Park 1989)

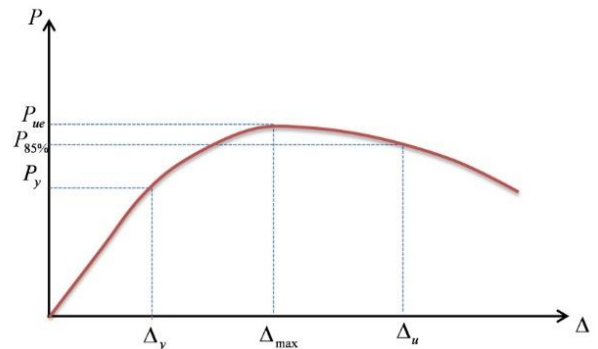


Fig. 5 Definition of ultimate displacement based on JGJ101-96

displacements, respectively. In this research, the methods presented schematically in Fig. 3(c) and Fig. 4(c) are employed to calculate the yield and ultimate displacements, respectively.

The JGJ101-96 instruction, by experimenting on the composite columns, considers the ultimate displacement of the corresponding point of 85% of base shear. Based on JGJ101-96, the used method for determination of the ultimate displacement is illustrated in Fig. 5.

## 2.2 Fiber hinge concept

One of the methods for modeling of the nonlinear responses of the components is to allocate the nonlinear response hinges with specified length to the places of the parts which are likely to show a nonlinear static response. The hinges have different types, but generally, from the cross-sectional modeling point of view, they are divided into two main categories (Kassaei *et al.* 2010):

1. The hinges which consider the entire cross section of the components as the points with characteristic geometry and material.
2. The hinges which divide the cross section of the components into smaller sub-components. Each of them has a length equal to the length of the hinge and the individual nonlinear loading and response.

The overall response of the component is determined according to the responses of the sub-component series. Each fiber could only undergo the longitudinal stress. Therefore, by means of these hinges, only the nonlinear responses of the components under the axial load and bending moment can be investigated. The force exerted to each fiber is the sum of the stresses times their allocated surface area on the main cross section. Actually, each fiber acts as a rod under the axial load. This type of modeling is known as fiber or layer theory or sometimes with other similar names.

In this research, based on the fiber theory and the combination of concrete and steel behaviors, the fiber plastic hinges are used.

## 2.3 Used stress-strain model of steel tube

The elastic-perfectly plastic model is considered for the behavior of steel tube, as shown in Fig. 6, where,  $\sigma_y$  represents the yield stress and  $E_s$  represents the elastic modulus (Hu *et al.* 2003).

## 2.4 Used stress-strain model of confined concrete

The model proposed by Lee *et al.* (2010) is used in the simulation of the confined concrete behavior. The full equivalent uniaxial stress-strain curve for confined concrete is divided into three parts as shown in Fig. 7. The first part of the curve is assumed to have an elastic range from zero to the proportional limit stress. The value of the proportional limit stress is taken as  $0.5f'_{cc}$  and the initial secant Young's modulus of confined concrete ( $E_{cc}$ ) is calculated through Eq. (5). The second part of the curve is the nonlinear portion, starting from proportional limit

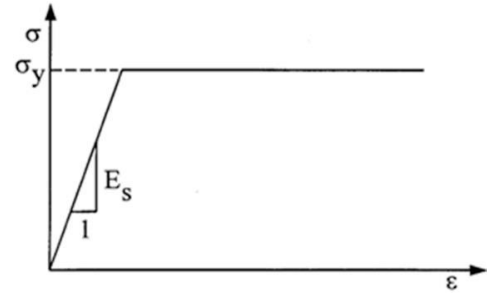


Fig. 6 Elastic-perfectly plastic model for steel tube (Hu *et al.* 2003)

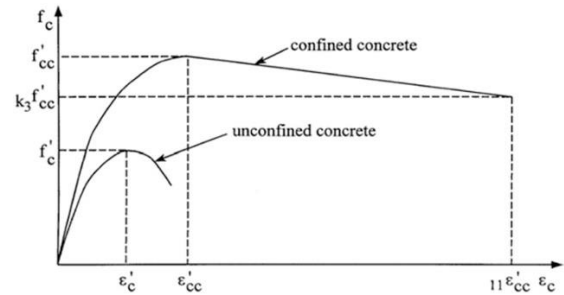


Fig. 7 Equivalent uniaxial stress-strain curve for confined concrete (Lee *et al.* 2010)

stress ( $0.5f'_{cc}$ ) and ending at the confined concrete strength ( $f'_{cc}$ ). Lastly, the third part of the curve is descending part of the confined concrete strength ( $f'_{cc}$ ) to a value lower than or equal to the corresponding strain of  $11\varepsilon'_{cc}$ . The stress-strain curve of confined concrete, which is calculated by Eq. (6), is illustrated in Fig. 7

$$E_{cc} = 5000\sqrt{f'_{cc}} \quad (5)$$

With

$$f'_{cc} = f'_c + K_1 f_1 \quad (6)$$

$$\varepsilon'_{cc} = \varepsilon'_c \left(1 + K_2 \frac{f_1}{f'_c}\right) \quad (7)$$

And with the following values:

$$K_1 = 4.1$$

$$K_2 = 5K_3$$

$$K_3 = 0.4 \quad \left(\text{when } 70 \leq \frac{B}{t} \leq 150\right)$$

$$K_3 = 0.000178\left(\frac{B}{t}\right)^2 - 0.02492\left(\frac{B}{t}\right) + 1.2722$$

$$\left(\text{when } 17 \leq \frac{B}{t} \leq 70\right)$$

$$f_1 = \left(0.055048 - 0.001885\left(\frac{B}{t}\right)\right)f_y$$

$$\left(\text{when } 17 \leq \frac{B}{t} \leq 29.2\right)$$

$$f_1 = 0 \quad \left(\text{when } 29.2 \leq \frac{B}{t} \leq 150\right)$$

Where:

- $f_i$ : lateral compressive stress by steel tube,
- $f'_{cc}$ : cylindrical strength of confined concrete,
- $f'_c$ : cylindrical strength of unconfined concrete,
- $\epsilon'_{cc}$ : strain of confined concrete at peak,
- $\epsilon'_c$ : strain of unconfined concrete at peak (0.003),
- $\frac{B}{t}$ : width to thickness ratio of the tube.

### 3. Numerical modeling

In this study, by employing SAP2000 software (Computers and Structures, Inc. 2010), 36 different steel MRFs with CFT columns were modeled and analyzed. All models assumed to have the same number of spans equal to 3 in each direction and also with dead and live loads of 5884 and 1961 Pa (600 and 200 kgf/m<sup>2</sup>), respectively. Furthermore, all models are designed based on AISC 360-05 (2005). In addition to that, all beams have IPE sections and all steel materials used in the column tubes and steel beams have a yield stress of 240 MPa. The modeled frames have 5, 10 and 15 stories. Each story in all of the models has 3-meter height and the span lengths are variable based on the specifications of the models.

Various models with different ratios of L/H of 1, 1.5 and 2, and the ratios of yield stress of steel to the compressive strength of core concrete ( $f_y/f'_c$ ) of 11.4, 9.6, 6.8 and 5 were examined. The introduced plastic hinges of these structures are fiber-interaction type in which the overall responses of the hinge would be obtained from the strain-stress response of each concrete or steel fiber. In Fig. 8, an example of the CFT column cross-section, divided into several fibers, is presented. Also, the ultimate lateral displacement was determined according to JGJ101-96 instruction.

Moreover, the naming of the models is done in a way that the first digit, indicates the number of stories, CMRF is the abbreviation of “composite moment-resisting frame”, the second digit shows the ratio of the L/H of the story and the last digit implies the ratio of  $f_y/f'_c$ .

To perform a static nonlinear analysis, using SAP2000 software, the combination of dead load and live load with a load factor of 1.1 for both dead and live loads is applied as gravitational design load. Loading, controlled by the



Fig. 8 CFT cross-section

Table 1 The properties of materials

Model name	Compressive strength of concrete (MPa)	Yield stress of steel (MPa)
15 & 10 & 5CMRF1-11.4	21.05	240
15 & 10 & 5CMRF1-9.6	25	240
15 & 10 & 5CMRF1-6.8	35.3	240
15 & 10 & 5CMRF1-5	48	240
15 & 10 & 5CMRF1.5-11.4	21.05	240
15 & 10 & 5CMRF1.5-9.6	25	240
15 & 10 & 5CMRF1.5-6.8	35.3	240
15 & 10 & 5CMRF1.5-5	48	240
15 & 10 & 5CMRF2-11.4	21.05	240
15 & 10 & 5CMRF2-9.6	25	240
15 & 10 & 5CMRF2-6.8	35.3	240
15 & 10 & 5CMRF2-5	48	240

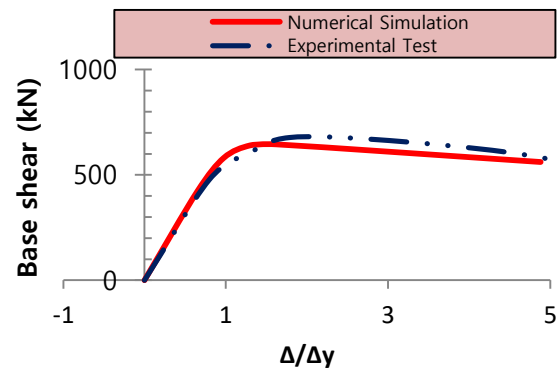


Fig. 9 Comparison of the results obtained from numerical simulation and experimental test

imposed force initiating from zero, and the triangular loading pattern, initiating from the above-mentioned gravitational load controlled by displacement, were employed (Instruction for seismic improvement in the existing buildings, 2006). The lateral deformation was exerted to the structure until the structure reached to the maximum displacement. Beyond the maximum displacement, the structure becomes unstable and the collapse happens. The properties of the applied materials are listed in Table 1.

#### 3.1 Validation of the proposed numerical nonlinear method

In order to verify the validity of the proposed numerical model, the response curve of a square shaped CFT column with high strength which was obtained from the static nonlinear numerical simulation using the proposed fiber-hinge model was compared to the results obtained experimentally by Varma *et al.* (2004) on the CFT columns under the constant axial loading and increasing lateral loading.

Fig. 9 demonstrates the numerical simulation result obtained by pushover analysis, compared to the

experimental test result of Varma (Varma *et al.* 2004). The comparison of the results shows a good agreement between the responses obtained applying the proposed numerical simulation and the experimental test response for both stiffness and strength, with a difference less than 5%.

#### 4. Ductility analysis and seismic response interpretation

Based on the nonlinear static analysis and application of plastic fiber-hinges, the pushover curves of a 5-story steel MRF with CFT columns and IPE cross-section beams were obtained. Figs. 10-12 depict the results obtained for different models and for the L/H ratios of 1.0, 1.5 and 2.0.

As a sample, the response of 5CMRF1-11.4 is described below. The pushover response of the mentioned model is classified, as illustrated in Fig. 13. The important phases on the response curve can be identified as listed below:

A: At this stage, the steel tube in the critical section of the column, reaches to yield stress; i.e., the first plastic-fiber is formed.

B: At this stage, the first steel beam reaches to yield stress and a plastic fiber-hinge is formed in it.

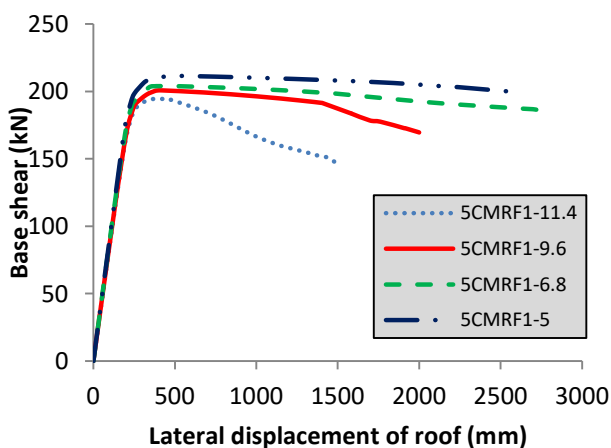


Fig. 10 Pushover curves, 5-story, L/H ratio of 1.0

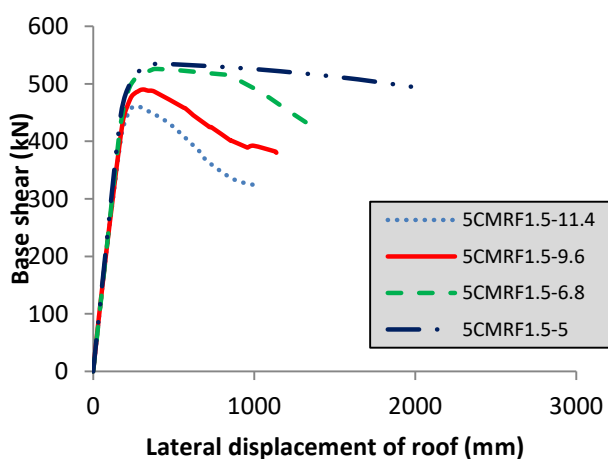


Fig. 11 Pushover curves, 5-story, L/H ratio of 1.5

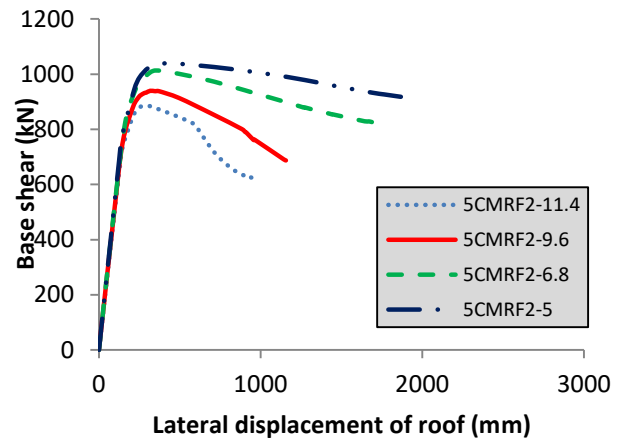


Fig. 12 Pushover curves, 5-story, L/H ratio of 2.0

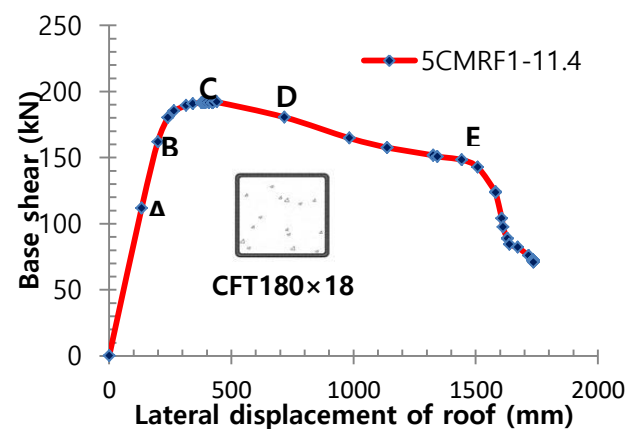


Fig. 13 Pushover curve of 5CMRF1-11.4 model

C: At this stage, the base shear reaches to its maximum value.

D: At this stage, the strain of filling concrete in the steel tube exceeds 0.033, and the degradation mechanism of the concrete is initiated.

E: At this stage, the steel tube fails.

To investigate the ductility, the pushover curves obtained from the static nonlinear analysis are idealized by a bilinear curve. In Fig. 14, the idealized bilinear curve adapted for the 5CMRF1-11.4 model is illustrated.

The ductility coefficient ( $\mu$ ), as well as the reduction coefficient due to the ductility ( $R_\mu$ ) and RMF ( $R$ ) of the steel MRFs with CFT columns can be computed, using the idealized bilinear curves. These parameters are submitted in Table 2. The obtained results, as shown in Table 2 and Figs. 10-12, indicate that, in the modeled MRFs, by increasing the compressive strength of the concrete, the ductility increases. Also, the lateral strength enhances due to the increasing the L/H ratio. In the cases of 5-story frames with  $f_y/f'_c$  ratios greater than 9, the ductility and as a result, the RMF considerably decreases. Generally, the optimized condition is achieved for the  $f_y/f'_c$  of about 7. Moreover, the average value of RMF for the steel MRFs with CFT columns with the L/H ratios of 1, 1.5 and 2 for a 5-story frame are equal to 8.38, 5.14, and 7.07, respectively. These

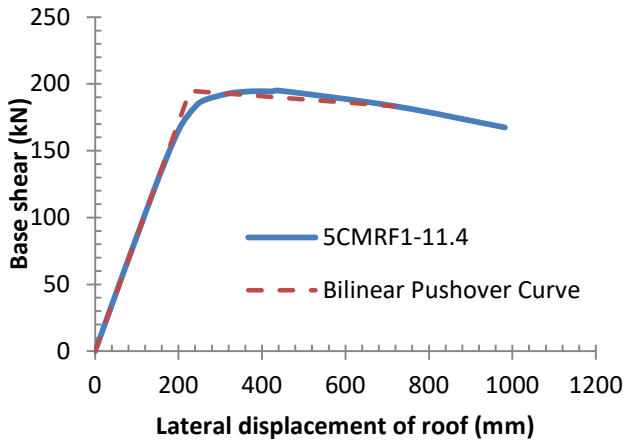


Fig. 14 Bilinear curve of 5CMRF1-11.4 model

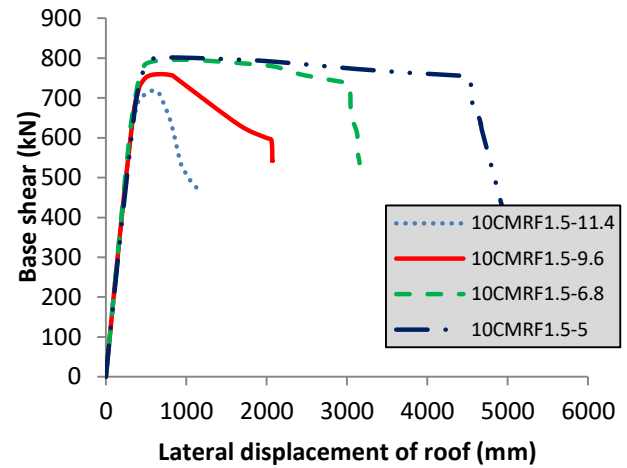


Fig. 16 Pushover curves, 10-story, L/H ratio of 1.5

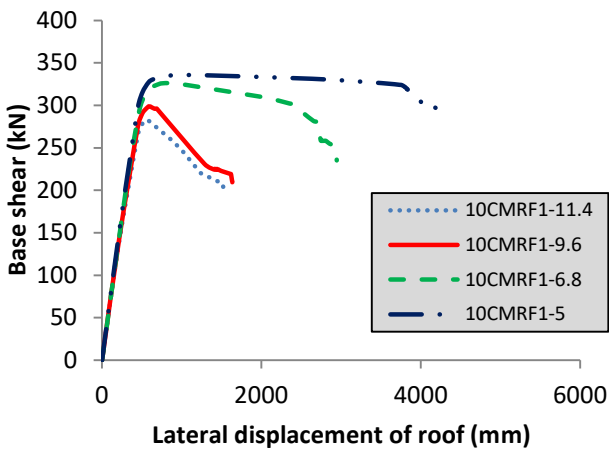


Fig. 15 Pushover curves, 10-story, L/H ratio of 1.0

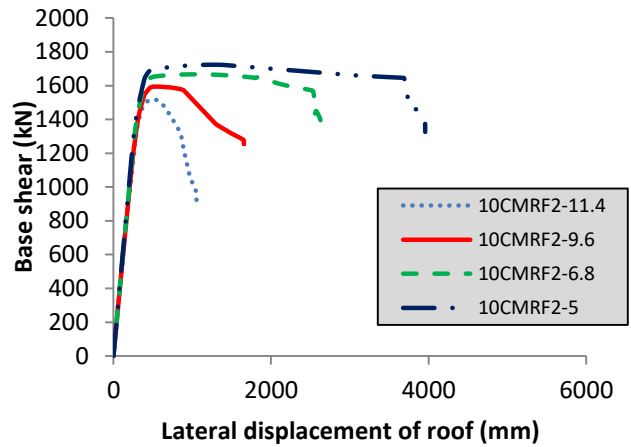


Fig. 17 Pushover curves, 10-story, L/H ratio of 2.0

Table 2 Seismic parameters of 5-story models

Models	$\mu$	$R_\mu$	$\Omega$	$R$
5CMRF1-11.4	4.18	3.03	1.77	5.37
5CMRF1-9.6	7.93	4.75	1.86	8.85
5CMRF1-6.8	11.92	6.35	1.67	10.06
5CMRF1-5	12.57	6.59	1.4	9.24
5CMRF1.5-11.4	3.55	2.71	1.06	2.88
5CMRF1.5-9.6	3.77	2.82	1.06	3
5CMRF1.5-6.8	5.61	3.72	1.37	5.11
5CMRF1.5-5	10.78	5.9	1.62	9.6
5CMRF2-11.4	3.49	2.67	1.48	3.95
5CMRF2-9.6	4.88	3.38	2.01	6.8
5CMRF2-6.8	6.99	4.34	2.04	8.88
5CMRF2-5	10.01	5.6	1.55	8.68

Table 3 Seismic parameters of 10-story models

Models	$\mu$	$R_\mu$	$\Omega$	$R$
10CMRF1-11.4	2.33	2.33	0.94	2.20
10CMRF1-9.6	2.35	2.35	1.00	2.35
10CMRF1-6.8	5.28	5.28	1.63	8.65
10CMRF1-5	8.24	8.24	1.16	9.55
10CMRF1.5-11.4	2.23	2.23	1.17	2.61
10CMRF1.5-9.6	4.26	4.26	1.94	8.26
10CMRF1.5-6.8	7.60	7.60	1.33	10.08
10CMRF1.5-5	10.95	10.95	1.12	12.27
10CMRF2-11.4	2.67	2.67	2.13	5.70
10CMRF2-9.6	3.77	3.77	1.53	5.79
10CMRF2-6.8	7.37	7.37	1.61	11.87
10CMRF2-5	10.89	10.89	1.24	13.48

values are close to the average values of the RMFs of the especial MRF given in ASCE-7-05 regulation (ASCE/SEI 7-05 2006). Therefore, the designers are recommended to use the RMFs of 8, 5 and 7 for the design of these frames with L/H ratios of 1, 1.5 and 2, respectively.

The pushover curves obtained for the examined 10-story

steel MRFs with CFT columns and IPE beams are depicted in Figs. 15-17.

The curves shown in Figs. 15-17, indicate that increasing the concrete compressive strength increases the ductility of the concrete. Moreover, by increasing the L/H ratio, the

lateral resistance arises. According to the results obtained for the ductility and RMF, shown in Table 3, it could be argued that in the 10-story frames with the  $f_y/f'_c$  ratios greater than 9, the ductility and as a result, the RMF shows a drastic reduction. In general, the optimized condition is achieved for the  $f_y/f'_c$  ratio of about 7. Also, the average value of RMF for the steel MRFs with CFT columns with the L/H ratios of 1, 1.5 and 2 are equal to 5.68, 8.30, and 9.21, respectively. These values are close to RMFs mentioned in ASCE-7-05 regulation for the especial MRFs (ASCE/SEI 7-05 2006). Therefore, the designers are recommended to use the RMFs of 6, 8 and 9 for the design of these frames with L/H ratios of 1, 1.5 and 2, respectively.

The obtained pushover curves of 15-story steel MRFs with CFT columns and IPE beams are depicted in Figs. 18-20.

Examining the Figs. 18-20, it can be concluded that in the modeled frames, by increasing the compressive strength of concrete, the ductility of the concrete increases. Furthermore, by increasing the L/H ratio, the lateral resistance increases as well. According to the obtained results for ductility and RMF, reflected in Table 4, it could

be concluded that in the 15-story frames with the  $f_y/f'_c$  ratios greater than 7, the ductility and as a result, the RMF sharply decreases. To sum up, the optimized condition is achieved for the  $f_y/f'_c$  ratio of about 5. Additionally,

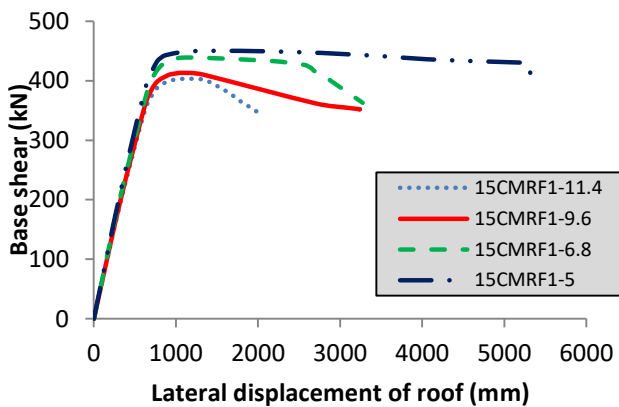


Fig. 18 Pushover curves, 15-story, L/H ratio of 1.0

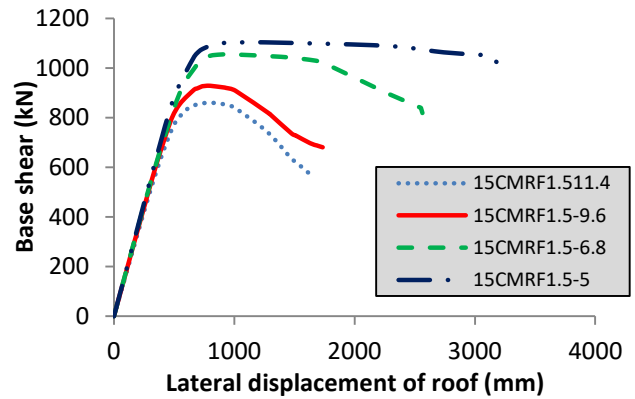


Fig. 19 Pushover curves, 15-story, L/H ratio of 1.5

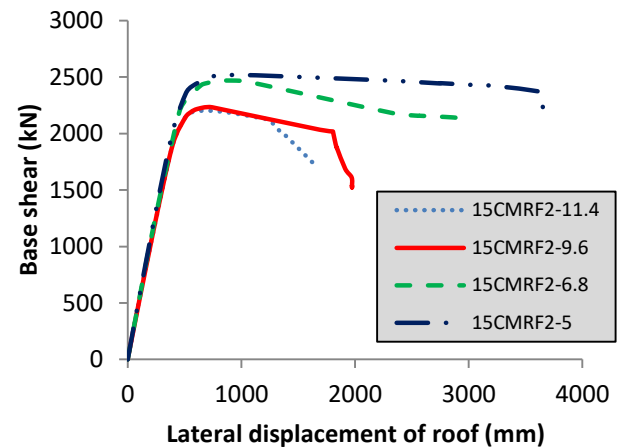


Fig. 20 Pushover curves, 15-story, L/H ratio of 2.0

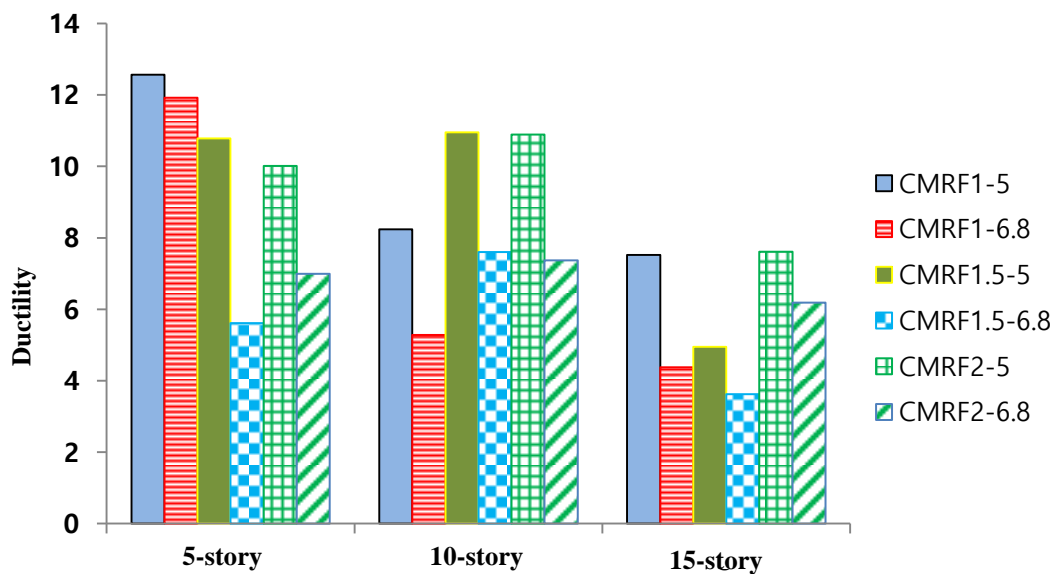


Fig. 21 The ductility of the 5-, 10- and 15-story structural models with CFT columns

Table 4 Seismic parameters of 15-story models

Models	$\mu$	$R_\mu$	$\Omega$	$R$
15CMRF1-11.4	2.95	2.95	1.10	3.27
15CMRF1-9.6	4.81	4.81	1.07	5.18
15CMRF1-6.8	4.38	4.38	1.12	4.93
15CMRF1-5	7.52	7.52	1.13	8.5
15CMRF1.5-11.4	2.39	2.39	1.70	4.07
15CMRF1.5-9.6	2.38	2.38	1.74	4.14
15CMRF1.5-6.8	3.62	3.62	2.01	7.28
15CMRF1.5-5	4.95	4.95	1.39	6.91
15CMRF2-11.4	3.24	3.24	1.16	3.79
15CMRF2-9.6	3.95	3.95	2.04	8.09
15CMRF2-6.8	6.19	6.19	1.04	6.47
15CMRF2-5	7.61	7.61	1.20	9.16

the average value of RMF for the steel MRFs with CFT columns with the L/H ratios of 1, 1.5 and 2 are equal to 5.47, 5.60, and 6.87, respectively. These values are close to the suggested value in ASCE-7-05 regulation for the RMFs of especial MRFs (ASCE/SEI 7-05 2006). Therefore, the RMFs of frames with L/H ratios of 1, 1.5 and 2 are proposed as 5, 6 and 7, respectively.

The investigation on the ductility of steel MRFs with CFT columns as reflected in Fig. 21, it is observed that in the frames with  $f_y/f_c'$  ratios less than 7 with L/H = 1, by increasing the number of the stories, the ductility decreases. Also, the ductility of the 5- and 10-story frames with the L/H ratios of 1.5 and 2 are close to each other and increasing the number of the stories to 15, this factor decreases.

## 5. Conclusions

In the present study, two important seismic parameters including, the ductility and response modification factor "RMF" ( $R$ ) of the MRFs with CFT columns are investigated. In addition to that, the effects of L/H ratio and the strength of materials on these parameters as well as, the seismic behavior are taken into consideration. The obtained results are listed as shown below:

- The ductility increases with the increase of concrete compressive strength.
- In the cases of low-rise and middle-rise frames with less than 10 stories, when the steel yield stress to concrete compressive strength ( $f_y/f_c'$ ) ratio exceeds the value of 9, the ductility and the RMF considerably decrease. Therefore, it is recommended that the CFT columns be designed for the  $f_y/f_c'$  ratios of less than 9.
- In the cases of high-rise frames with about 15 stories, when the  $f_y/f_c'$  value exceeds 7, the ductility and the RMF considerably decrease. Therefore, it is recommended that the CFT columns be designed for the  $f_y/f_c'$  ratios of less than 7.
- The obtained RMFs for 5-story frames as low-rise

frames with L/H ratios of 1, 1.5 and 2, are 8, 5 and 7, respectively. These values are close to the average value of the RMF of the composite MRF given in ASCE-7-05.

- The obtained RMFs for 10-story frames as middle-rise frames with L/H of 1, 1.5 and 2, are 6, 8 and 9, respectively. These values are close to the average value of the RMF of the composite MRF given in ASCE-7-05.

- The obtained RMFs for 15-story frames with L/H ratios of 1, 1.5 and 2, are 5, 6 and 7, respectively. These values are close to the average value of the RMF of the composite MRF given in ASCE-7-05.

- The 5-story models with an L/H ratio of 1, have higher ductility and RMF in comparison with L/H ratios of 1.5 and 2.

- The 10-story models with an L/H ratio of 1.5 have higher ductility and RMF values in comparison with L/H ratios of 1 and 2.

- The 15-story models with an L/H ratio of 2, have higher ductility and RMF values in comparison with L/H ratios of 1 and 1.5.

## References

- ANSI/AISC 360-05 (2005), Specification for Structural Steel Building, American Institute of Steel Construction, Chicago.
- ASCE/SEI 7-05-2006 (2006), Minimum Design Loads for Buildings and Other Structures, American Society of Civil Engineers, New York.
- Building Seismic Safety Council (2001), NEHRP, *Recommended Provisions for Seismic Regulations for New Buildings and Other Structures (FEMA 450)*: Provisions/Prepared by the Building Seismic Safety Council, National Institute of Building Sciences, Washington.
- Computers and Structures, Inc. (2010), SAP 2000 advanced 14.2.0, Berkeley, California, USA.
- Esfandyary, R., Razzaghi, M.S. and Eslami, A. (2015), "A parametric investigation on the hysteretic behaviour of CFT column to steel beam connections", *Struct. Eng. Mech.*, **55**(1), 205-228.
- Evirgen, B., Tuncan, A. and Taskin, K. (2014), "Structural behavior of concrete filled steel tubular sections (CFT/CFSt) under axial compression", *Thin-Wall. Struct.*, **80**, 46-56.
- Han, L.H., Wang, W.D. and Zhao, X.L. (2008), "Behavior of steel beam to concrete-filled SHS Column frames: finite element model and verifications", *Eng. Struct.*, **30**(6), 1647-1658.
- Hu, H.T., Huang, C.S., Wu, M.H. and Wu, W.M. (2003), "Nonlinear analysis of axially loaded concrete-filled tube columns with confinement effect", *J. Struct. Eng.*, **129**(10), 1322-1329.
- JGJ101-96 (1996), *Chinese Specification of Testing Methods for Earthquake Resistant Building*, Architecture Industrial Press of China, Beijing.
- Jiango, N., Kai, Q. and Yan, X. (2006), "Push-over analysis of the seismic behavior of a concrete-filled rectangular tubular frame structure", *Tsinghua Sci. Technol.*, **11**(1), 124-130.
- Karamis, G.S., Skalomenos, K.A., Hatzigeorgiou, G.D. and Beskos, D.E. (2016), "Seismic damage estimation of in-plane regular steel/concrete composite moment resisting frames", *Eng. Struct.*, **115**, 67-77.
- Kassaei, A., Pourzeiali, S. and Ghaffari, E. (2010), "The effect of the number of defined fibers in the plastic hinges on the dynamic non-linear response of the steel buildings", *5<sup>th</sup> National Congress on Civil Engineering*, Mashhad, Iran. (in

Persian)

- Kuranovas, A. and Kvedaras, A.K. (2007), "Behavior of hollow concrete-filled steel tubular composite elements", *J. Civ. Eng. Manage.*, **13**(2), 131-141.
- Kwon, Y.B. and Jeong, I.K. (2014), "Resistance of rectangular concrete-filled tubular (CFT) sections to the axial load and combined axial compression and bending", *Thin-Wall. Struct.*, **79**, 178-186.
- Lee, S.H., Uy, B., Kim, S.H., Choi, Y.H. and Choi, S.M. (2010), "Behavior of high-strength circular concrete-filled steel tubular (CFST) column under eccentric loading", *J. Constr. Steel Res.*, **67**(1), 1-13.
- Long, Y.L., Wan, J. and Cai, J. (2016), "Theoretical study on local buckling of rectangular CFT columns under eccentric compression", *J. Constr. Steel Res.*, **120**, 70-80.
- McCormack, J.C. (2007), *Structural Steel Design (LRFD Method)*, Harpercollins College Div, Mishawaka, India.
- Nateghi Elahi, F. (2008), "An experimental investigation of concrete filled tube columns (CFST) ductility", *Scientific Res. J. Struct. Steel*, **3**(5), 3-12. (in Persian)
- Park, R. (1989), "Evaluation of ductility of structures and structural assemblages from laboratory testing", *Bull. NZ. Nat'l Soc. Earthq. Eng.*, **22**(3), 155-166.
- Park, T., Hwang, W.S., Leon, R.T. and Hu, J.W. (2011), "Damage evaluation of composite-special moment frames with concrete-filled tube columns under strong seismic loads", *KSCE J. Civ. Eng.*, **15**(8), 1381-1394.
- Pokharel, T., Yao, H., Goldsworthy, H.M. and Gad, E.F. (2016), "Experimental and analytical behaviour of cogged bars within Concrete Filled Circular Tubes", *Steel Compos. Struct.*, **20**(5), 1067-1085.
- Schneider, S.P. and Kramer, D.R. (2004), "The design and construction of concrete-filled steel tube columns frames", *13<sup>th</sup> World Conference on Earthquake Engineering*, Vancouver, August.
- Tasnimi, A.A. and Masoumi, A. (2006), *Calculation of Armed Concrete Moment Resisting Frames' Response Modification Factor*, Research Center of Building and Houses, Tehran, Iran. (in Persian)
- The management and planning organization of country (2006), *Instruction for Seismic Improvement in the Existing Buildings of Country*, the technical affairs office of measures establishment and reducing the risk of earthquakes, Tehran. (in Persian)
- Varma, A.H., Ricles, J.M., Sause, R. and Lu, L.W. (2004), "Seismic behavior and design of high-strength square concrete-filled steel tube beam columns", *J. Struct. Eng.*, **130**(2), 169-179.
- Wan, C.Y. and Zha, X.X. (2016), "Nonlinear analysis and design of concrete-filled dual steel tubular columns under axial loading", *Steel Compos. Struct.*, **20**(3), 571-597.
- Xiamuxi, A., Hasegawa, A. and Yu, J. (2015), "A study on nonlinear analysis and confinement effect of reinforced Concrete Filled Steel tubular column", *Struct. Eng. Mech.*, **56**(5), 727-743.
- Xiao, Y., He, W., Mao, X., Choi, K.K. and Zhu, P. (2005), "Confinement design of CFT columns for improved seismic performance", *J. Struct. Eng.*, **131**(3), 488-497.
- Zhang, D., Gao, S. and Gong, J. (2012), "Seismic behaviour of steel beam to circular CFST column assemblies with external diaphragms", *J. Constr. Steel Res.*, **76**, 155-166.